



# PHOTOLUMINESCENCE, MICROSTRUCTURE AND ELECTRICAL PROPERTIES OF $\text{CuInSe}_2$ THIN FILMS

D. S. Patil<sup>1</sup>, S. B. Patil<sup>2</sup>, P. H. Pawar<sup>3\*</sup>

<sup>1</sup>S. S. M. M. Arts, Science and Commerce College, Pachora-424201, Maharashtra, India

<sup>2</sup>Dr. S.D.D. Art's College, Commerce and Science College, Wada, Dist.; Palghar -421303, Maharashtra, India

<sup>3\*</sup>Z. B. Patil Arts, Science and Commerce College, Dhule- 424 002, Maharashtra, India.

**Abstract:** This work focus on the synthesis and characterization of  $\text{CuInSe}_2$  thin films by chemical bath deposition technique on glass substrate. After annealed of thin films were use for further characterization of different analytical techniques including EDAX, XRD, FESEM, TEM and SAED pattern. Optical properties were carried out by using UV-spectroscopy and photoluminescence measurements respectively. Electrical properties were conducted using two probe method and TEP measurement set up. The obtained results were interpreted and discussed.

**Keywords:** Nancube  $\text{CuInSe}_2$  thin films, Photoluminescence, Chemical Reaction

\* Corresponding author E-mail: [sharadpatil123@yahoo.co.in](mailto:sharadpatil123@yahoo.co.in)

## 1. INTRODUCTION

In the last 3-4 decades semiconducting Chalcogenides thin films have found various applications in diverse fields of science and technology. The optical property of thin films is also very important in many scientific, technological, and industrial applications and numerous other applications [1].

The semiconductor interface used for the construction of photo electrochemical cells has been the subject of intensive research [2]. Amongst these, the semiconductors  $\text{CuInS}_2$  and  $\text{CuInSe}_2$  are highly sensitive to light and other radiation because of this, the study of different properties of their mixed thin film structures is of technical and scientific importance. The chemical bath deposition method of preparation of thin films is very simple. It requires solutions of exact morality and quantity. One of these compounds,  $\text{CuInSe}_2$ , with its optical absorption coefficient exceeding  $3 \times 10^4 \text{ cm}^{-1}$  at wavelengths below 1000 nm, and its direct band gap being between 0.95 and 1.04 eV, is an excellent solar. Thin film polycrystalline CIS solar cells with a conversion

efficiency exceeding 14% have already been achieved. High absorption coefficient and low cost methods for deposition of thin films make  $\text{CuInSe}_2$  a promising material for photovoltaic devices.

The  $\text{CuInSe}_2$  thin films were prepared on glass substrates using chemical bath deposition techniques. This heterostructure of firmly adherent films is useful for solar absorbers solar devices control and other important applications. The chemical bath deposition is relatively inexpensive, simple and convenient for large area deposition. Various semiconducting materials have been prepared by the solution growth technique. Since the exact measurement can give the accurate value of pH of solution.

Various deposition techniques, have been employed to prepare  $\text{CuInSe}_2$  thin films including flash evaporation [3], single source evaporation [4], multiple source evaporation molecular beam epitaxy [5], spray pyrolysis [6], and electrodeposition [7]. Chemical bath deposition is a method of growing thin films of certain materials on a substrate immersed in an aqueous bath containing appropriate reagents at temperatures ranging from room temperature to 100 °C. It has been identified as a low process suitable for the preparation of large area thin films [8].

Chemical bath deposition method has attracted much attention since it is conformed as a simple and promising technique to obtain device quality films. CBD is a simple which is also used to deposit the semiconductor on photovoltaic device. The CBD method appears suitable for large area industrial process because it is the least expensive and a low temperature method [9].

The deposited films samples were characterized by XRD, FESEM, AFM, EDAX, TEM, SAED pattern, UV-spectroscopy, Photoluminescence, and electrical properties. This work investigates effect of Cu/In ratio on physical, structural, micro structural, electrical and optical properties of these thin films were discussed. The results were discussed and interpreted in the present investigation.

## 2 EXPERIMENTAL PREPARATION OF NANOCUBE $\text{CuInSe}_2$ THIN FILMS

In the present study, the chemicals used for the synthesis of  $\text{CuInSe}_2$  thin films are; cupric chloride dihydrate ( $\text{CuCl}_2 \cdot 2\text{H}_2\text{O}$ ) [purity 98%, Astron Chemicals, India], indium(III) chloride anhydrous ( $\text{InCl}_3$ ) [purity 99.99%, Alfa Aesar, A Johnson Matthey Company, U.S.A], triethanolamine (TEA) ( $\text{C}_6\text{H}_{15}\text{NO}_3$ ) [purity 99%, Astron Chemicals, India], elemental selenium (Se) [purity 99%, SISCO Chem Pvt. Ltd., Mumbai, India], sodium sulfite ( $\text{Na}_2\text{SO}_3$ ) [purity 98% Alfa Aesar, A Johnson Matthey Company, U.S.A] and hydrochloric acid (HCl) (35% pure)[10].

. All the chemicals were of AR grade and were used as received without any processing or purification. All chemicals were stored in evacuated desiccators to prevent degradation due to atmosphere or humidity.

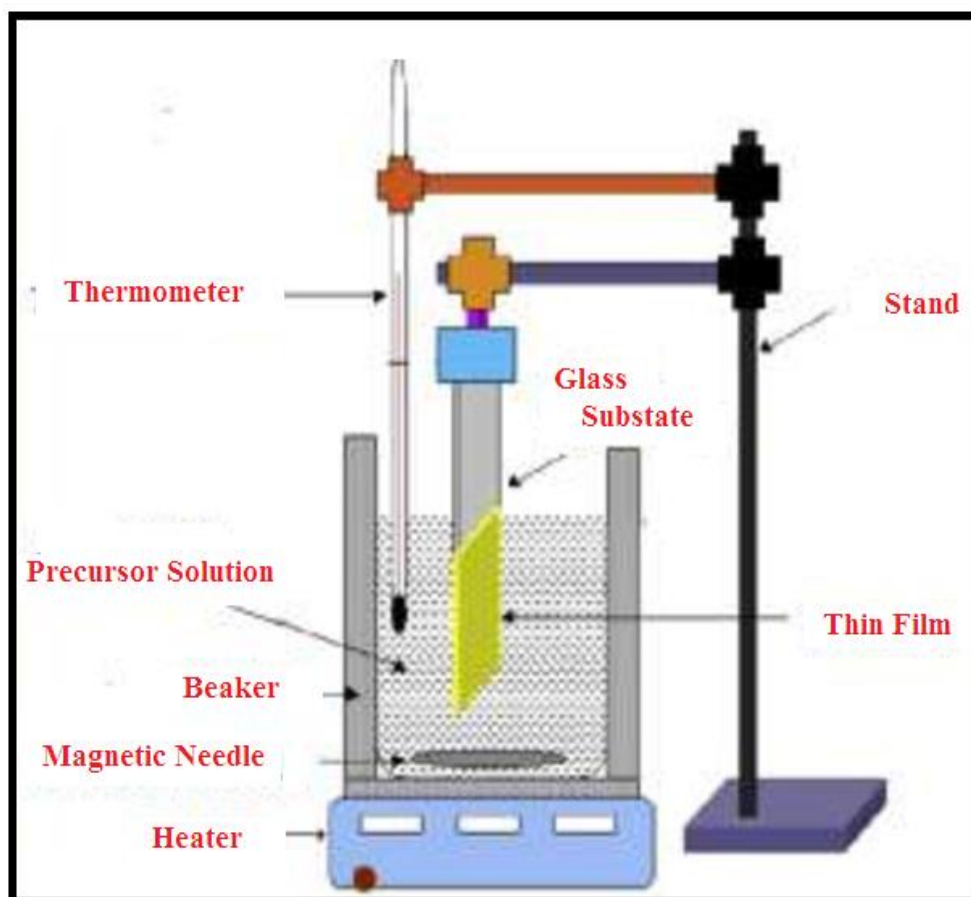


Figure 1: Experimental set up of Chemical bath deposition technique

Starting solutions were prepared by dissolving requisite amount of respective elements in double distilled water. The  $\text{Cu}^{2+}$  ion solution was prepared using  $\text{CuCl}_2 \cdot 2\text{H}_2\text{O}$  and  $\text{In}^{3+}$  ion solution was prepared by  $\text{InCl}_3$ . The  $\text{Se}^{2-}$  ion solution was prepared using  $\text{Na}_2\text{SO}_3$  and elemental Se. The 1 M  $\text{Na}_2\text{SeSO}_3$  was prepared by refluxing 7.90 g of elemental Se with 12.60 g of  $\text{Na}_2\text{SO}_3$  in 100 ml of double distilled water for 8 h at 90 °C temperature. The reaction leading to the formation of  $\text{Na}_2\text{SeSO}_3$  is;



The TEA ( $\text{C}_6\text{H}_{15}\text{NO}_3$ ) acts as a complexing agent to control the slow release of ions so that immediate agglomeration does not happen. The HCl is added to set the pH of the solution 9. After preparation of above precursor solutions, deposition of  $\text{CuInSe}_2$  thin films was carried out as below.

The solution for the deposition of  $\text{CuInSe}_2$  thin film by CBD technique was prepared by firstly taking 5 ml of 0.5 M  $\text{CuCl}_2 \cdot 2\text{H}_2\text{O}$  solution in a 100 ml clean dry glass beaker. To it was added 5 ml of 0.1 M TEA ( $\text{C}_6\text{H}_{15}\text{NO}_3$ ) solution. The addition was done under continuous magnetic stirring and continued for 5 min. Then to the mixture, 5 ml of 0.5 M  $\text{InCl}_3$  was added.

The addition was done under continuous stirring. The stirring was carried out for 10 min. After that 5 ml of 1 M  $\text{Na}_2\text{SeSO}_3$  was mixed slowly under stirring. Lastly, 5 ml of 0.1 M HCl was added to the mixture and stirred for 5 min. At last 50 ml of double distilled water was added to make the final solution 75 ml in volume.

The pH of the final bath solution was measured and was found to be 4. The pre-cleaned glass slide substrate was immersed in the bath solution and kept vertical in the beaker containing final solution for thin film deposition to occur. The glass slide substrates used for deposition were laboratory grade glass slides having

dimensions as  $76 \text{ mm} \times 26 \text{ mm} \times 1 \text{ mm}$  [Blue Star, Delhi, India]. The procedure adopted for cleaning of the glass slides was; firstly the slides were thoroughly washed with detergent and dried in air.

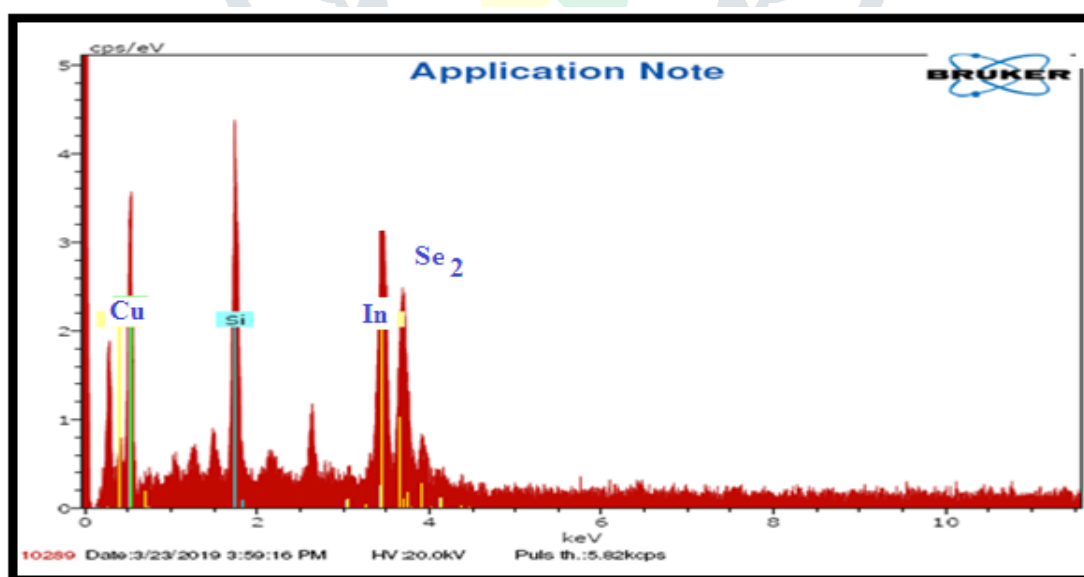
The air dried slides were then dipped in concentrated hydrochloric acid and were kept immersed for 24 h. After 24 h acid dip, the slides were removed and were given multiple wash with double distilled water. The water was allowed to drain off and the slides were air dried. The perfectly dried slides were finally given ultrasonication in acetone for 10 min.

Lastly, the glass slides were kept in an oven by maintaining it at  $80^\circ\text{C}$  till used for deposition of thin films. The deposition was carried out at room temperature for 3 h. The glass slide with deposited thin film was removed from the solution, rinsed with double distilled water and allowed air drying. The as prepared  $\text{CuInSe}_2$  thin film samples were fired at  $350^\circ\text{C}$  for 10 min. After cooling of samples at room temperature prepared thin films were use for further characterization and electrical with optical properties.

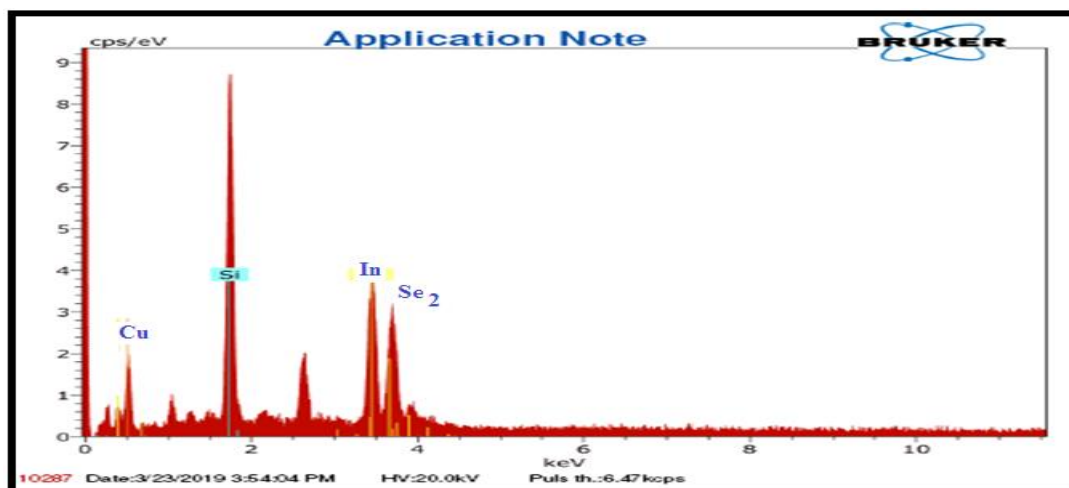
### 3. CHARACTERIZATIONS OF THIN FILMS

#### 3.1 EDAX Spectra of Nanocube Thin Film

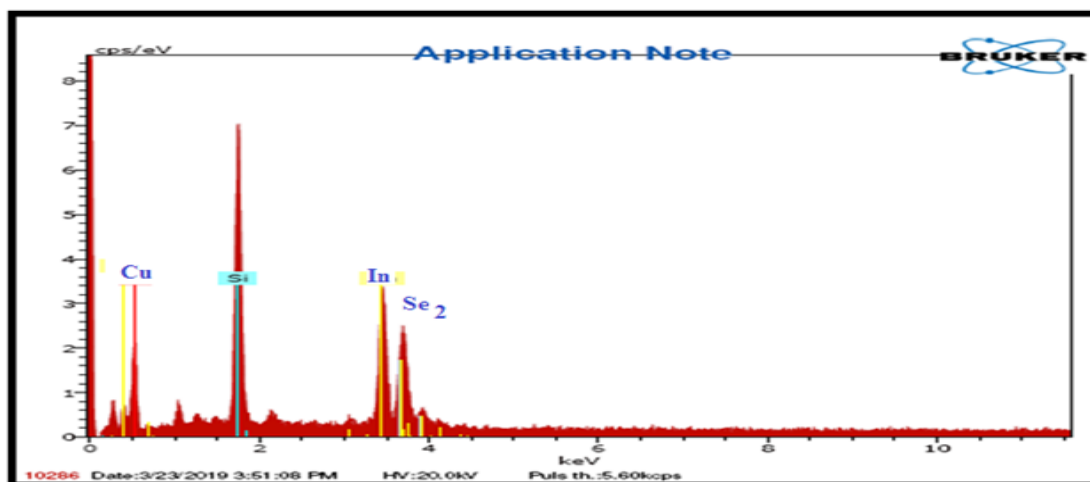
The atomic compositions of the grown thin films on glass substrate at room temperature have been determined by Energy dispersive analysis of X-ray (EDAX) method. Table 1 shows the elemental composition of the thin films from EDAX. Theoretically expected stoichiometric composition of  $\text{CuInSe}_2$  (in terms of at %) is: Cu = 25%, In=25% and Se=50% .



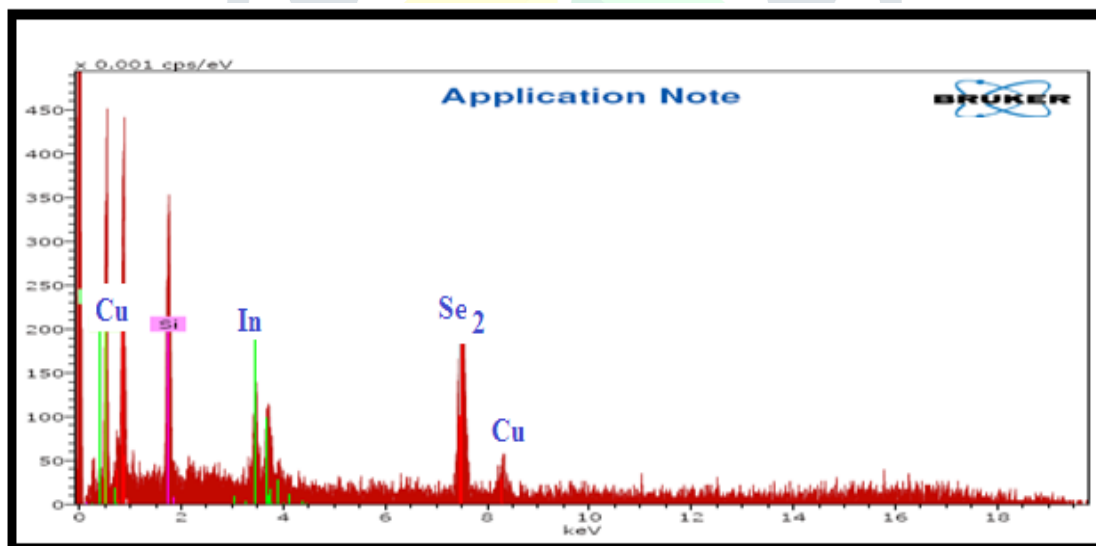
D1



D2



D3



D4

**Figure 2: EDAX spectra of CuInSe<sub>2</sub> thin film for samples D1, D2, D3 and D4.**

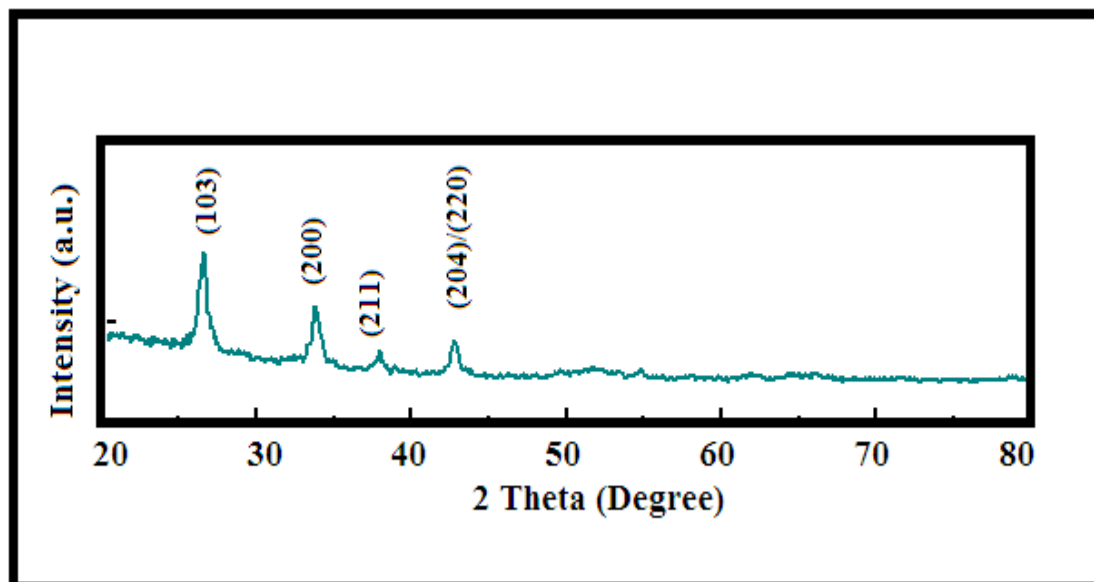
Figure 2 (D1 to D4) depicts the EDAX spectra of CuInSe<sub>2</sub> thin films as different at % of Cu/In ratio.

Table 1: Elemental composition of nanocubes CuInSe<sub>2</sub> thin films

Sample Number	at % of the elements in film				wt % of the elements in film			
	Cu	In	Se	Cu/In	Cu	In	Se	Cu/In
D1	27.22	23.45	49.33	1.11	37.23	23.12	39.65	1.61
D2	32.65	26.42	40.93	1.23	40.12	19.67	40.21	2.03
D3	42.23	13.69	44.08	3.08	42.69	17.65	39.66	2.41
D4	47.22	12.69	40.09	3.72	51.69	14.55	33.76	3.55

It is clear from Table 1 that the films are observed to be nonstoichiometric in nature.

### 3.2 Structural Properties



**Figure 3: X-ray diffractogram of CuInSe<sub>2</sub> thin film for samples D3**

The analysis of the XRD pattern was done by powder-X software. Figure 3 show the X-ray diffractogram of pattern of the film. It shows presence of different strong diffraction peaks. Thin film sample D3 was scanned in the  $2\theta$  range of 20–80°. All the diffraction peaks could be indexed to be that of CuInSe<sub>2</sub> having tetragonal unit cell structure. The broadness in the XRD pattern appears due to the nanocrystalline thin film. The lattice parameters  $a$  and  $c$  calculated from the XRD patterns of the CBD as-deposited CuInSe<sub>2</sub> thin film came out to be 5.782 Å and 11.621 Å respectively.

All the indexed peaks and the determined lattice parameters were in good agreement with the standard data vide JCPDS Card Number: 40-1487. The XRD also confirmed that the CBD as-deposited thin film possess single phase CuInSe<sub>2</sub>, as no other binary phase nor non indexed peaks were observed.

The  $c/2a$  lattice parameter ratio calculated for the CBD as-deposited CuInSe<sub>2</sub> thin film came out to be ~ 1.005, which is within the reported values of 1.003–1.008 [23,24], thus further confirming the single phase of CuInSe<sub>2</sub>.



The value of tetragonal distortion  $\Delta = 2 - c/a$  came out to be  $-0.009$ , the negative sign indicates compression. From the full-width at half-maximum of the diffraction peaks, the average crystallite sizes of the  $\text{CuInSe}_2$  have been calculated using the Debye-Scherrer formula [11]. Estimated average crystallite sizes found to be in the range of 14 nm.

### 3.3 Surface morphology studies using FE-SEM

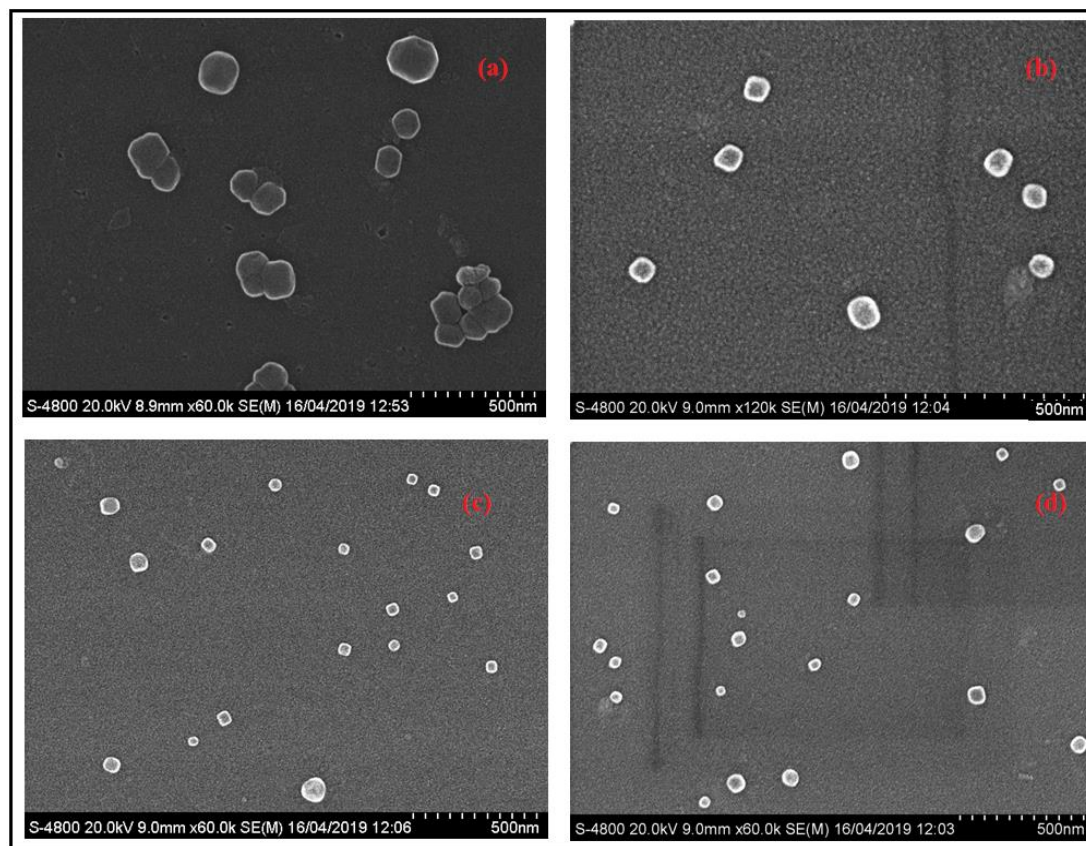


**Figure 4:** (a), (b), (c), and (d) FESEM images of the nanocubes  $\text{CuInSe}_2$  thin sample.

Fig. 4 depicts the FESEM surface topography of the film samples with different Cu/In ratios. We could observe a uniformly distributed growth of cubic-shaped  $\text{CuInSe}_2$  nanocrystals. The FESEM images show that the thin film surface is uniform and smooth without any major features. The film surface is continuous without any cracks stating the deposition to be homogeneous all throughout the substrate surface. It is noted that for the film formed without aging of precursor solution exhibit clear and smooth grains. Such cubic morphology makes this nanomaterial a good candidate for the production of solar cell, photovoltaic cell [12].

Estimated grain sizes ranged from 31 nm to 49 nm. Grain size decreased with the rise in at% of Cu and In ration from 1.11 to 3.72. FESEM images revealed that the grain number increased with an increase in the at ratio of Cu/In, which may be attributed to increase in grain size.

Further, we also observed expansion of larger grains to smaller grains, a characteristic of the nucleation stage. Surface diffusion plays a key role in  $\text{CuInSe}_2$  growth process, in which the particles translocate to adjacent surface sites; this movement increases with increase in at ratio [13].

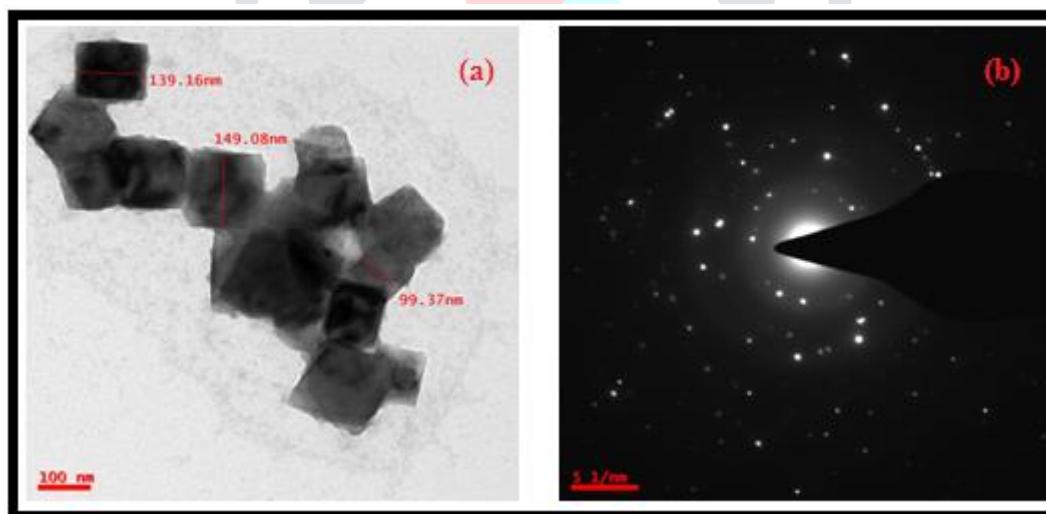
The  $\text{CuInSe}_2$  films that deposit on the substrate do not possess adequate energy for the formation of the crystalline structure owing to less at ratio. Increase in at ratio results increase in the thermal energy that is necessary for the process of crystallization.

**Table 2:** Dependence of grain size on Cu/In ratio.

Sample No.	Figure 2	Cu (at.%)/ In (at.%)	Grain size (nm)	Shape of grains
D1	a	1.11	49	Spherical and Cubic
D2	b	1.23	43	Cubic
D3	c	3.08	37	Cubic
D4	d	3.72	31	Cubic

It is clear from (Table 2) FESEM images that the number of grains goes on increasing with the increase in Cu/In ratio. Also, with the increase in at % of Cu there is a decrease in average grain size. It could be attributed to small atomic radii of Cu ions as compared to indium. Smaller the atomic radii, larger would be the nucleation centres and smaller would be the grains. The amount of feed material available in the reaction vessel is constant for a particular reaction. If same material would be divided on the larger nucleation centres, the grain would not grow larger but remain smaller [13].

### 3.4 Microstructured studies using Transmission electron micrograph and SAED pattern

**Figure 5:** (a-b) TEM and SAED pattern of nanowires CuInSe<sub>2</sub> thin sample D3

The analysis of the micrograph image shows that the substrate is well covered by the deposited CuInSe<sub>2</sub> thin film. We further used the TEM to examine the crystal structure of CuInSe<sub>2</sub> nanocubes. The obtained images depicted the particles to be cubic on surface (Fig. 5 (a)). Analysis of all TEM images indicated of uniform cubic nanostructure with average particle size ~129 nm.

Fig. 5 (b) depicts the SAED pattern of CuInSe<sub>2</sub> (D3). The surface electron diffraction patterns show clear and spotty continuous ring patterns indicating a polycrystalline structure [14].



### 3.5 Optical Properties Study Using UV-Spectroscopy

The optical energy band gap of CuInSe<sub>2</sub> thin film was estimated from optical absorption measurement. Fig. 6 shows the variation of relative absorbance with wavelength for nanostructured CuInSe<sub>2</sub> thin films. The optical absorption spectrum for the CuInSe<sub>2</sub> thin film is recorded in the wavelength range of 400–1400 nm at room temperature shown in Fig. (6).

The band gap energy calculated from absorbance spectra are 1.72, 1.91, 2.43, 2.55 eV of samples D1, D2, D3 and D4 respectively. The reported band gap energy of nanostructured CuInSe<sub>2</sub> thin films samples was 1.39 eV [15]. Optical band gap energy was observed to be large as compared to reported work it may be due to formation of nanocrystalline thin films.

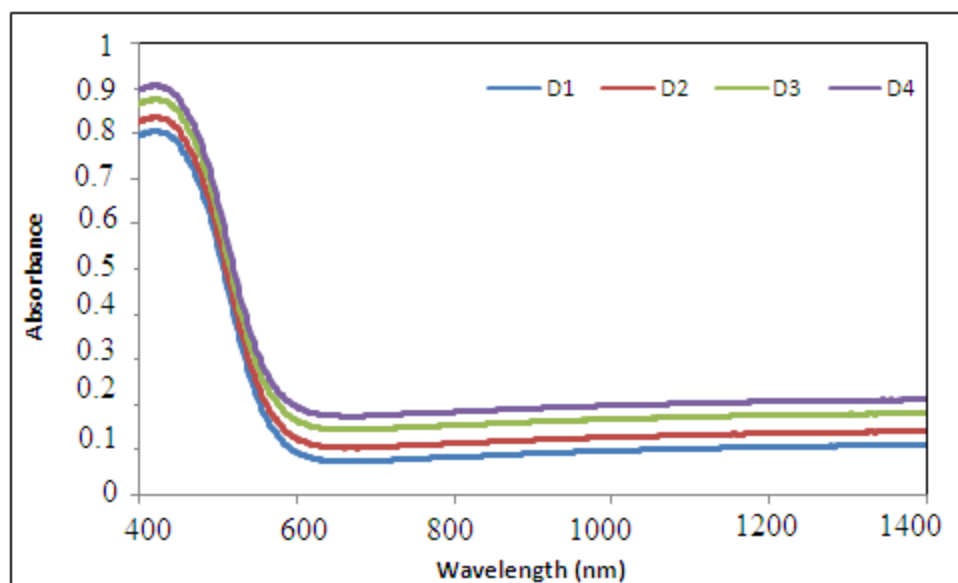


**Figure 6:** Absorbance spectra of as deposited nanocubes CuInSe<sub>2</sub> thin sample for different at % of Cu and In

The band gap energy is the most important parameter in semiconducting thin film material. It is reasonably affected by deposition conditions [16-18]. This suggests the decrease in the band gap energy ( $E_g$ ) with increasing at ration of Cu/In. It is strongly observed that the CuInSe<sub>2</sub> thin films exhibit the least reflectance for almost all wavelengths. From the above studies, it is believed that the CuInSe<sub>2</sub> thin films may be used as an antireflection coating material for thin film solar cell [19].

Figure 7 shows the variation of optical band gap energy with Cu/In (at%) ratio. It is clear from the graphs that the values of band gap energy go on increasing with the increase in Cu/In ratio.

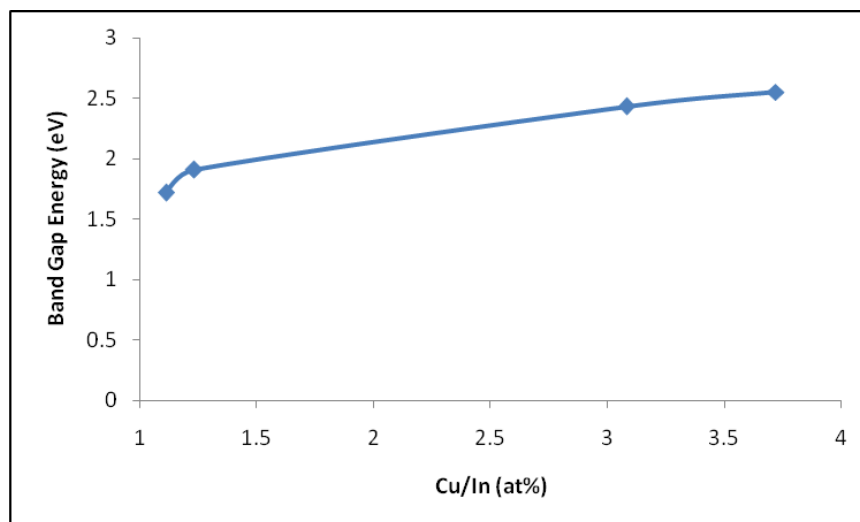


**Figure 7: Dependence of Cu/In (at%) ratio and optical band gap energies (eV).**

### 3.6 Measurement of film thickness

Surface profiler (AMBIOS Tech. (USA) XP.I; vertical resolution: 1.5 Å, lateral length: 200 nm, and lateral resolution: 100 nm) was used to measure the thin film thickness.

The measured thickness of the thin film samples D1, D2, D3, and D4 were observed to be 390 nm, 721 nm, 641 nm, and 436 nm respectively. Thickness was observed to be randomly it would be due to different at % of Cu/In ratio.

### 3.7 Photoluminescence (PL) spectra of CuInSe<sub>2</sub>

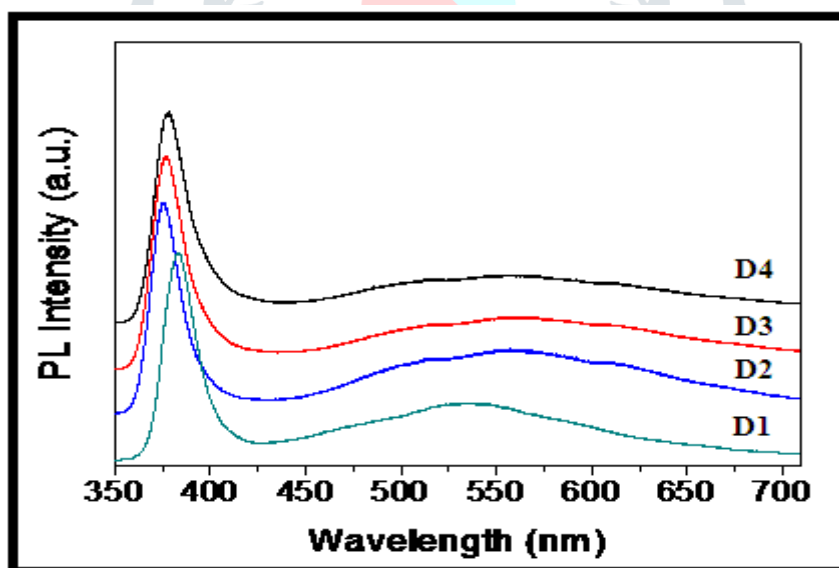


**Figure 8: Photoluminescence spectra (PL) nanocubes CuInSe<sub>2</sub> thin sample for different at % of Cu and In.**

Fig. 8 shows room temperature PL spectra of the nanocubes CuInSe<sub>2</sub> of samples (D1, D2, D3 and D4) measured using Xenon laser of 300 nm as excitation source.

The spectra of each nanocubes CuInSe<sub>2</sub> thin film samples D1, D2, D3 and D4 mainly consist of two emission peaks: (i) a strong UV emission peak at 360 to 380 nm, (ii) a weak peak at 450 nm and 468 nm,

4. ELECTRICAL PROPERTIES

4.1. Measurement of electrical conductivity and activation energy

➤ Electrical conductivity

Conductivity was given by relation:

$$\sigma = \sigma_o \exp (- \Delta E/kT) \text{ ----- (2)}$$

Where,  $\sigma$  = conductivity  
 $\sigma_o$  = conductivity constant  
 $k$ = Boltzmann constant  
 $T$ = Temperature.

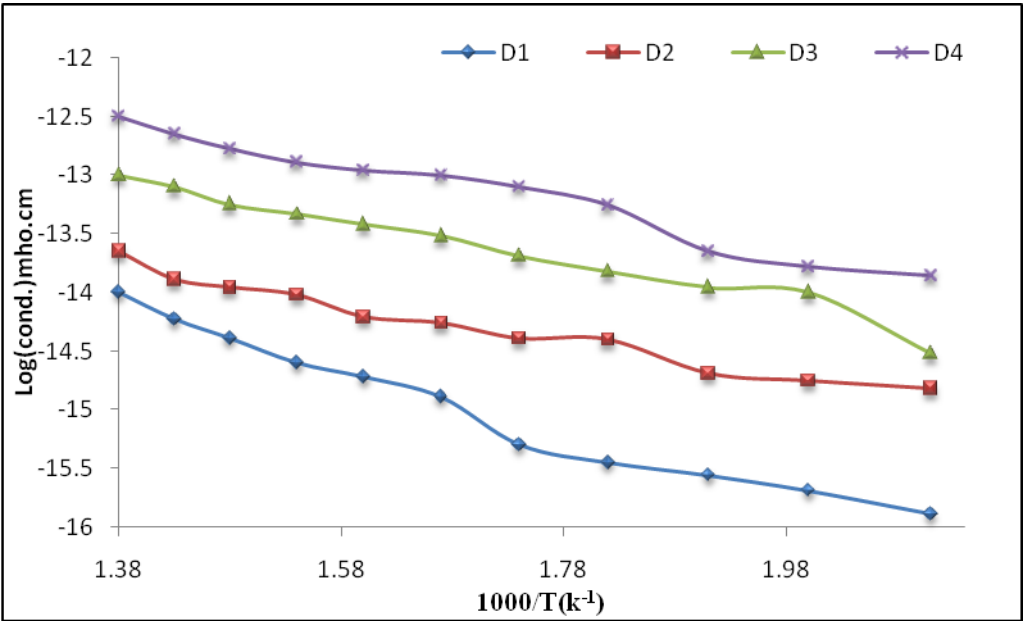


Figure 9: Variation of log (σ) with 1000/T (k<sup>-1</sup>)

The conductivity of each sample is observed to be increasing with an increase in temperature. The increase in conductivity with increase in temperature could be attributed to negative temperature coefficient of resistance and semiconducting nature of nanocubes CuInSe<sub>2</sub>. Variation of conductivity with operating temperature Fig (9) clearly indicates that the pure nanocubes CuInSe<sub>2</sub> films are semiconducting in nature.

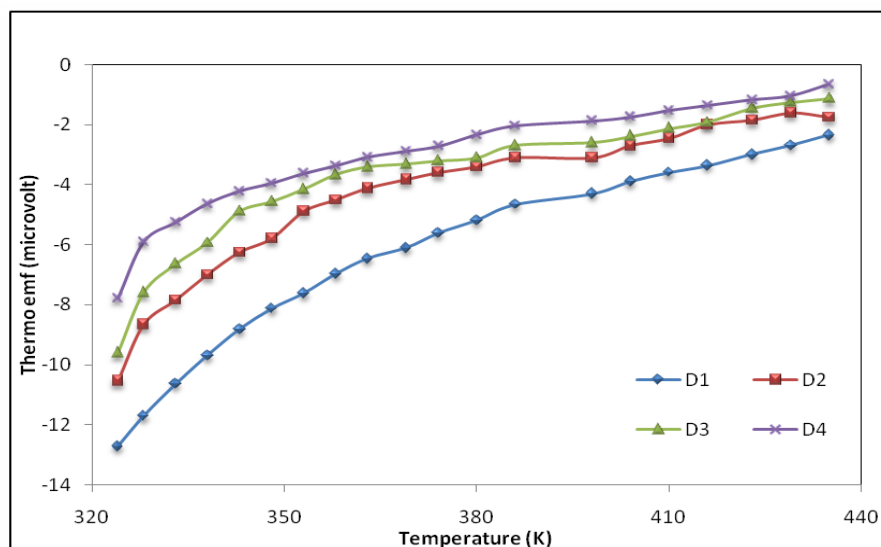
Table 3 enlists the activation energies calculated from the slopes of logarithm of conductivity versus inverse of temperature.

Table 3: Measurement of Cu/In ratio of the sample and activation energy.

Sample No.	Cu/In	Activation energy (ΔE)	
		298 K (Low Temperature)	423 K (High Temperature)
D1	1.11	0.56 eV	0.23 eV
D2	1.23	0.47 eV	0.21 eV
D3	3.08	0.41 eV	0.17 eV
D4	3.72	0.33 eV	0.14 eV

Previous studies have reported that activation energy varies with the at ratio of Cu/In. Our findings supported this notion, as shown in Table 3. Previous studies have also reported an inverse correlation between activation energy and sizes of grains and crystallites [20].

#### 4.2. Thermo emf measurement



**Figure 10: Thermo emf vs Temperature ( $^{\circ}\text{K}$ ) of nanocubes  $\text{CuInSe}_2$  thin films.**

In order to decide the type of charge carrier, thermoelectric measurement was taken. The graph of TEP Vs Temperature (K) is as shown in Fig (10). In the thermo emf measurement the temperature difference causes the transport of carriers from hot end to cold end and thus creates an electric field which gives thermal voltage. This thermally generated voltage is directly proportional to the temperature difference created across the semiconductor.

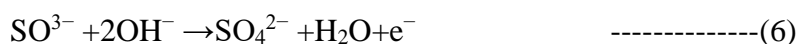
TEP is the ratio of thermally generated voltage to the temperature difference across the semiconductor. Diffusion of thermally generated majority charge carriers occurs from high temperature to the low temperature end, as a result of temperature difference ( $\Delta T$ ). This creates a positive space charge near high temperature end, which sets up an electric field or potential difference thereby giving rise to a thermal emf ( $\Delta E$ ) [21].

The polarity of the thermo emf was positive at the hot end with respect to the cold end which conformed that  $\text{CuInSe}_2$  films are of  $n$ - type. The thermo emf was measured as a function of temperature in the range between 50 and 150  $^{\circ}\text{C}$ . The variation of the thermo emf with temperature difference for all the samples is shown in Figure (9).

#### 5 DISCUSSION:

The separate cationic precursor solution consisted of two parts: the copper precursor solution was 0.05 M  $\text{CuCl}_2 \cdot 2\text{H}_2\text{O}$  and the indium precursor solution was 0.05 M  $\text{InCl}_3$ . The anionic source for selenium was 0.1 M  $\text{Na}_2\text{SeSO}_3$  solution. The pH of the solution was maintained at 4 by addition of 0.1 M of HCl. The HCl is a strong acid which dissociates fully and helps in reaction bath protonation. Here TEA acts as a complexing agent to ensure slow release of Cu ions in the deposition mixture.

The base constant  $K_b$  of TEA is  $5.75 \times 10^{-7}$  at ambient temperature [22] meaning that the nitrogen atoms of TEA are substantially protonated by hydrogen ions in the pH region of the present reaction condition. The formation or complexing constant of  $[\text{Cu}(\text{TEA})_2]^{2+}$  is  $1 \times 10^6$  [16], stating to be too high. In the chemical bath,  $\text{Cu}^{2+}$  ions released from the  $[\text{Cu}(\text{TEA})_2]^{2+}$  were reduced to  $\text{Cu}^+$  ions due to the presence of excess sodium sulfite according to below reactions [23,24]:



$\text{Se}^{2-}$  ions are released from the sodium selenosulphate solution:



The excess sodium sulfite over selenium prevents the oxidation of selenium and facilitate in re-precipitation as selenium [25]. The overall reaction for the formation of  $\text{CuInSe}_2$  is thus,



## 6. CONCLUSION

Nanocubes  $\text{CuInSe}_2$  thin films were prepared by simple and inexpensive chemical bath deposition technique. The chlorides of copper,  $\text{CuCl}_2$ , and indium,  $\text{InCl}_3$ , were used as Cu and In precursors, whereas Se source was sodium seleno sulphate ( $\text{Na}_2\text{SeSO}_3$ ). The triethanolamine ( $\text{C}_6\text{H}_{15}\text{NO}_3$ ) and hydrochloric acid,  $\text{HCl}$ , were used as complexing agent and for adjusting pH of the deposition solution, respectively. The structural, surface morphological and micro-structural properties confirm that the as-prepared  $\text{CuInSe}_2$  thin films are nanocrystalline in nature. XRD study confirms phase of  $\text{CuInSe}_2$ . The elemental analysis conformed that as prepared thin films were nonstoichiometric in nature. TEM and SAED pattern analysis confirms the nanostructured properties and development of  $\text{CuInSe}_2$  with the help of simple chemical bath deposition technique. As the at ratio of Cu/In changes, crystalline size and grain size goes on increasing while activation energy goes on decreases. Electrical conductivity of the nanocrystalline  $\text{CuInSe}_2$  thin films were observed to be increased with increase in temperature. TEP measurement indicate that as prepared  $\text{CuInSe}_2$  thin films were *n*-type in nature.



## 7. ACKNOWLEDGEMENTS

*The authors are thankful to Head, Department of Physics and Principal, Z. B. Patil Arts, Science and Commerce College, Dhule for providing laboratory facilities for this work. Thanks to Principal, S. S.M.M. College, Pachora for his encouragement.*

## REFERENCES

- [1] Zinoviev, K.V., Zeleya-Angel, O., Materials Chemistry and Physics, 70 (2001), 100-102
- [2] K. D. Dobson, I. Visoly-Fisher, G. Hodes, and D. Cahen, Solar Energy Materials & Solar Cells, 62 (2000), 295-325
- [3] Elliot E, Tomlinson R D, Parkes J and Hampshire M J 1974 *Thin Solid Films* **20** S25
- [4] Kazmerski L L 1979 *Thin Solid Films* 58 29
- [5] Nealkanth G, Dhere M, Lourence C, Ramesh G, Dhere G and Kazmerski L L 1984 *Solar Cells* **13** 59
- [6] Grindle S P, Clark A H, Falconer E, Neily M and Kazmerski L L 1980 *J. Appl. Phys.* **51** 5664
- [7] Agnihotri O P, Rajaram P, Thangaraj R, Sharma A K and Raturi A 1983 *Thin Solid Films* **102** 291
- [8] Al-Bassam A A I 1999 *Physica* **B266** 192
- [9] S.A. Mahmoud, A.A. Ibrahim, A.S. Riad, *Thin Solid Films*, 372 (2000) 144-148
- [10] S. M. Chauhana, S. H. Chaki, M.P. Deshpande, J. P. Tailor, A. J. Khimani, Materials Science in Semiconductor Processing 74 (2018) 329–335
- [11] R. H. Bari and S. B. Patil, International Journal of Chemical Concepts, Vol.02, No.02, pp 88-95, 2016
- [12] S.H. Chaki, M.P. Deshpande, J.P. Tailor, Thin Solid Films 550 (2014) 291–297.
- [13] R. H. Bari, L. A. Patil, P P Patil, Bull. Mater. Sci., Vol. 29, No. 5, October 2006, pp. 529–534.
- [14] R. H. Bari, S. B. Patil, A.R. Bari, G. E. Patil, J. Aambekar, Sensors & Transducers Journal, 140 (2012) 124-132.
- [15] S.H. Chaki, M.D. Chaudhary, M.P. Deshpande, J. Semicond. 37 (2016)053001–053009.
- [16] R. Devi, P. Pukayse, Indian Journal of Pure and Applied Physics, (July 2007) Vol.45, 1624-627
- [17] R. H. Patil, S. N. Patil, S. V. Nikam and B. P. Ladgaonkar International Journal of Advances in Engineering & Technology, May 2013, 692 Vol. 6, Issue 2, 688-695
- [18] Ruby Das, Suman Pandey. International Journal of Material Science vol.1, Issue1, 2011, 35-40
- [19] S. S. Kavar, K. K. Hunde, A. P. Pachkawade, B. H. Pawar, International Journal of Basic and Applied Research, 2012, NC RTP, 157-160
- [20] G.K. Williamson, W.H. Hall, Acta Metall. 1 (1953) 22–31.
- [21] S. B. Patil, R. H. Bari, Archives of Physics Research (Scholars Research Library), 2014, 5 (6), 1-11.
- [22] T.J. Whang, M.T. Hsieh, Y.C. Kao, S.J. Lee, Appl. Surf. Sci. 255 (2009) 4600–4605.
- [23] S.H. Chaki, M.P. Deshpande, J.P. Tailor, Thin Solid Films 550 (2014) 291–297.
- [24] M. Lakshmi, K. Bindu, S. Bini, K.P. Vijayakumar, C.S. Kartha, T. Abe, Y. Kashiwaba, Thin Solid Films 370 (2000) 89–95.
- [25] M. Dhanam, R. Balasundaraprabhu, S. Jayakumar, P. Gopalakrishnan, M.D. Kannan, Phys. Status Solidi 191 (2002) 149–160.